Inorganic Chemistry

Article

pubs.acs.org/IC

Formation of Double-Strand Dimetallic Helicates with a Terpyridine-Based Macrocycle

Carla Bazzicalupi,[†] Antonio Bianchi,*[,†] Tarita Biver,[‡] Claudia Giorgi,[†] Samuele Santarelli,[§] and Matteo Savastano[†]

[†]Department of Chemistry "Ugo Schiff", University of Florence, Via della Lastruccia 3, 50019 Sesto Fiorentino, Italy

[‡]Department of Chemistry and Industrial Chemistry, University of Pisa, Via Moruzzi 3, 56124 Pisa, Italy

[§]Eni S.p.A., Centro Ricerche per le Energie non Convenzionali, Istituto Eni-Donegani, Via G. Fauser 4, 28100 Novara, Italy

Supporting Information

ABSTRACT: The macrocyclic ligand (L), containing two terpyridine (terpy) and two ethylenediamine (en) groups arranged in a cyclic terpy-en-terpy-en sequence, forms a double-strand helicate Cu_2L^{4+} complex made especially stable by the formation of interstrand $\pi-\pi$ stacking interactions involving opposite pyridine rings. The crystal structure of this complex shows the Cu^{2+} cations in square pyramidal coordination environments defined by the donor atoms of half ligand chain composed, in sequence, by one pyridine ring, the connected ethylenediamine moiety and the two adjacent pyridine rings of the successive terpyridine. In aqueous solution, L forms both mono- and binuclear complexes with Cu^{2+}. The stability constants determined for these complexes evidence the combined action of the two metal ions in the assembly of the very stable helicate species, the binding of the first metal ion favoring the entrance of the second one. UV adsorption and emission spectra corroborate these equilibrium results. Furthermore, the Cu_2L^{4+} complex shows a significant inertness toward dissociation in acidic solutions. Also Zn^{2+} forms mono- and binuclear complexes with L, although the Zn_2L^{4+} complex is much weaker than the Cu_2L^{4+} helicate and gives rise to fast dissociation reactions in acidic media. Experimental evidence allows neither to say that also the Zn^{2+} complex has a helicate structure nor to exclude it.

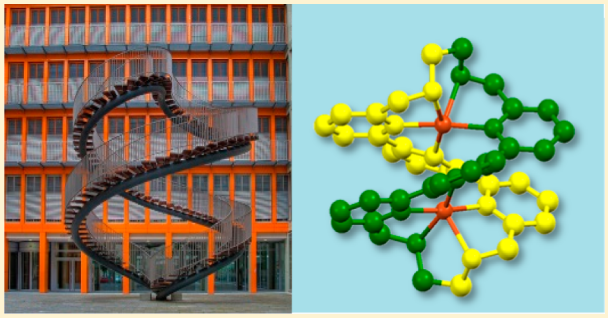

INTRODUCTION

Until the late 1980s, terpyridine was an unusual tridentate ligand mainly used for the colorimetric determination of metal ions[1,2] and for occasional coordination studies.[3−5] From the successive decade, however, it was recognized as a pivotal component for the construction of molecular devices[6,7] and supramolecular assemblies,[8] and accordingly it received a great deal of interest. It was incorporated in a variety of sophisticated derivatives and used for a wide number of applications. Just to make a few examples, terpyridine groups were incorporated into polymers, dendrimers, and nanotubes; they were used for surface functionalization, for the construction of molecular devices and machines, for the preparation of compounds with antitumoral activity, and for applications in nuclear medicine and magnetic resonance.[9,10]

The vast majority of terpyridine applications are related to its binding properties toward transition metal ions. The most typical coordination motif of this ligand is represented by the $[M(terpy)_2]^{n+}$ complexes in which two almost planar terpyridine molecules are nearly perpendicular to each other around the metal center in a distorted octahedral geometry. Commonly, terpyridine forms fairly stable $[M(terpy)_2]^{n+}$ metal complexes, but in the case of transition metals that are particularly favored by the octahedral geometry, like Fe(II) that undergoes high spin−low spin transition upon coordination of the second ligand molecule, complex stability can be very high. Furthermore, in contrast to bidentate ligands (L−L) that give rise to chiral $[M(L-L)_3]^{n+}$ species, the $[M(terpy)_2]^{n+}$ motif is achiral. Accordingly, coordination of two terpyridine derivatives to a metal ion can afford a firm connection for the assembly of extended structures giving rise, when the terpyridine derivatives have symmetric structures, to single species instead of isomeric mixtures. All these properties make terpyridine a predictable building block for the design of metal-based architectures endowed with chemical robustness, thermodynamic and kinetic stability, fundamental characteristics that have been used for the development of controlled molecular motion in rotaxanes,[11−15] for the assembling of catenanes,[16,17] molecular knots,[18] doubly threaded rotaxanes,[19] for two-ring threading,[20] and for the preparation of several macrocyclic complexes used for a variety of applications.[21−43] Terpyridine was also employed in the preparation of helicates[44−51] although most of these complexes were not based on the typical $[M(terpy)_2]^{n+}$ octahedral motif,

Received: September 25, 2014
Published: November 4, 2014

but they involved Cu^{+} or Ag^{+} ions in lower coordination numbers.[46−51] Interestingly, it was shown that combining tridentate terpyridine (T) with bidentate bipyridine (B) units affords TT and TB pairs suitable for selective assembling of Zn^{2+} and Fe^{2+} or Cu^{2+} helicates, respectively, according to the coordination preferences of the metal ion.[44,45]

A few years ago, we reported the synthesis of the macrocyclic polyamine L (Figure 1a), its binding properties in solution

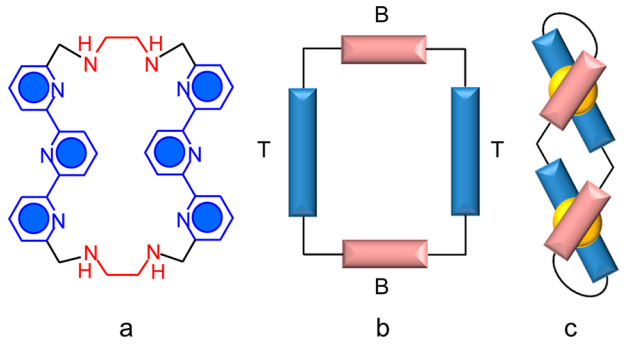

Figure 1. (a) The L ligand. (b) A schematic representation of the sequence of tridentate (T) and bidentate (B) binding sites. (c) A hypothetical double-strand helicate arrangement achieved upon coordination of two metal ions.

toward the nucleotide thymidine 5′-triphosphate (H_5TTP), and the crystal structure of the [(H_4L)HTTP] adduct.[31] Since this molecule contains four distinct donor sites, namely, two terpyridine and two ethylenediamine units, L is a good candidate for the formation of polynuclear complexes. As a matter of fact, it has been shown that polyamine macrocycles containing aromatic or heteroaromatic groups may give rise to polynuclear complexes with special coordination features, even when the ligand is small and contains a reduced number of donor atoms.[52−55] Furthermore, the alternate arrangement within the macrocyclic ring of tridentate terpyridine (T) and bidentate ethylenediamine (B) units furnishes the correct TBTB sequence of chelating units (Figure 1b) for the assembling of an intramolecular double helicate binuclear complex (Figure 1c). Taking into account the flexibility of the ethylenediamine chains and the rotational freedom of terpyridine rings, the achievement of a similar structure seemed possible despite the relatively small dimension of the macrocycle.

With this in mind, we studied the coordination properties of L toward Cu^{2+} and Zn^{2+} and, successfully, we observed the formation of a very stable double helicate Cu_2L^{4+} complex, both in solution and in the solid state, although the effective TBTB sequence of chelating units appeared to be different from the one shown in Figure 1. We report here the results of this study.

EXPERIMENTAL SECTION

General Information. Unless otherwise specified, all starting materials were purchased from commercial sources and used as supplied. The ligand L was obtained as L·6HBr according to a previously reported synthetic procedure.[31] The $Cu_2L(ClO_4)_2\cdot 0.33DMSO\cdot 0.33[Na_2OH(H_2O)(ClO_4)_7]$ complex (DMSO = dimethyl sulfoxide) was obtained by mixing together a warm water solution of L at pH 8, containing the minimum amount of DMSO required to dissolve the ligand, with a warm solution containing the appropriate amount of $Cu(ClO_4)_2$ in water. A gentle warming was maintained for a few minutes, then the solution was allowed to cool to room temperature, and its pH was again adjusted to 8 by using a dilute NaOH solution. Deep blue crystals of the complex, suitable for X-ray analysis, formed upon slow evaporation at room temperature. ***Caution!*** *Perchlorate salts of metal complexes are potentially explosive. Only a small amount of material should be prepared, and should be handled with care.*

Potentiometric Measurements. Potentiometric (pH-metric) titrations, used to determine the complex stability constants, were performed in 0.1 M NMe_4Cl at 298.1 ± 0.1 K by using an automated apparatus and a procedure previously described.[56] The combined Metrohm 6.0262.100 electrode was calibrated as a hydrogen-ion concentration probe by titration of previously standardized amounts of HCl with CO_2-free NaOH solutions and determining the equivalent point by Gran's method,[57] which gives the standard potential E° and the ionic product of water (pK_w = 13.83(1) in 0.1 M NMe_4Cl at 298.1 K). The computer program HYPERQUAD[58] was used to calculate the complex stability constants from the potentiometric data. Because of the low competition between ligand protonation and metal ion coordination, titrations were performed in the presence of ethylenediaminetetraacetic acid (EDTA). The concentration of the ligand was 5×10^{-4} M, the concentration of the metal ion (M) was varied in the range of $[L] \leq [M] \leq 3.5[L]$, and the concentration of EDTA was 1.5[L]. The studied pH range was 2.5−11. Nevertheless, because of the low solubility of L and HL^{+}, ligand precipitation was observed above pH 7 for sample solutions with low concentration of metal ion, but the acidic branches of these titrations were used for the determination of the stability constants. Because of some slowness observed in the attainment of equilibrium condition during Cu^{2+} complexation titrations, 10 min were allowed to elapse between titrant additions for this metal ion. Longer times were demonstrated to be superfluous. Four measurements were performed for both Cu^{2+} and Zn^{2+}. For each system, the titration curves were treated as a unique set in the calculation of stability constants. The hydrolysis of metal ions was taken into account in calculations. Ligand protonation constants used in calculation were previously reported.[31] Protonation and complexation constants for EDTA were taken from the literature.[59] Because of the low solubility of L and HL^{+}, the ligand was defined as H_2L^{2+} in calculations, and the equilibria involving the formation of complexes with the ligand in lower protonation states were set as deprotonation processes. Different equilibrium models for the complex systems were generated by eliminating and introducing different species. Only those models for which the HYPERQUAD program furnished a variance of the residuals $\sigma^2 \leq 9$ were considered acceptable. Such condition was unambiguously met by a single model for each system.

Spectrophotometric and Spectrofluorimetric Measurements. Absorption spectra were recorded at 298 K on a Jasco V-670 spectrophotometer, and fluorescence emission spectra were recorded on a PerkinElmer LS55 spectrofluorimeter. Kinetic measurements involving the dissociation of the binuclear Cu^{2+} complex in acidic solutions were performed at different pH by monitoring the variation with time of the UV spectrum of the Cu_2L^{4+} complex (2×10^{-5} M, pH 7) after addition of appropriate amounts of a concentrated HCl solution. The initial rate (0.71−1.4 pH range) was measured as the slope of the initial part of the kinetic trace. The correct pH of the solutions was measured at the end of the dissociation experiments and was assumed to be constant during the entire process due to the large excess of H^{+} ions relative to ligand concentration. Owing to these pseudo-first-order conditions, the kinetic traces could be analyzed also according to exponential functions (concentration = $Ae^{-t/\tau}$). The exponential analysis is done provided that the absorbance versus time signal is transformed into a complex concentration (conc) versus time signal (t). The procedure uses the absorbance data at the end of the kinetic process (spectra recorded 1 d after mixing) and the equation $y = (A - A_\infty)/(\varepsilon_{in} - \varepsilon_\infty)$, where ε_{in} is the initial molar extinction coefficient of the undissociated complex ($\varepsilon_{in} = A_{in}/C_L$) and ε_∞ is the molar extinction coefficient of the totally dissociated complex ($\varepsilon_\infty = A_\infty/C_L$). This procedure is done only in the cases where 100% of the initial binuclear complex is supposed to dissociate to a unique mononuclear form (0.71−1.0 pH range). The ionic strength of the solutions was kept constant at 0.22 M by suitable addition of NaCl.

X-ray Structure Analyses. A summary of crystallographic data for $Cu_2L(ClO_4)_2\cdot0.33DMSO\cdot0.33[Na_2OH(H_2O)(ClO_4)_7]$ is reported in Table 1. The integrated intensities were corrected for Lorentz and polarization effects, and empirical absorption correction was applied.[60] The structures were solved by direct methods (SIR92).[61] Refinements were performed by means of full-matrix least-squares using SHELX-97 program.[62] All non-hydrogen atoms were anisotropically refined, while the hydrogen atoms linked to the carbon atoms and nitrogen atoms were introduced in calculated positions, and their coordinates were refined according to the linked atoms. The perchlorate anion bridging the sodium ions, as well as the DMSO cocrystallized solvent, were disordered and localized in two different positions treated with sight occupation factor fixed at 0.5. Additional crystallographic data are available in the Supporting Information.

Table 1. Crystal Data and Structure Refinement for $Cu_2L(ClO_4)_2\cdot0.33DMSO\cdot0.33[Na_2OH(H_2O)(ClO_4)_7]$

empirical formula	$C_{58}H_{60}Cl_{6.5}Cu_3N_{15}NaO_{27.5}S_{0.5}$
formula weight	1867.28
temperature (K)	100
space group	*C*2/*c*
a (Å)	36.131(2)
b (Å)	20.2539(4)
c (Å)	28.625(2)
β (deg)	137.78(1)
volume (Å^3)	14 075.8(1)
Z	8
independent reflections/*R*(int)	13 492/0.0475
μ (mm^{-1})	4.365 (Cu K*α*)
R indices [$I > 2\sigma(I)$][a]	*R*1 = 0.0563
	w*R*2 = 0.1489
R indices (all data)[a]	*R*1 = 0.0762
	w*R*2 = 0.1733

[a] $R1 = \Sigma||F_o| - |F_c||/\Sigma|F_o|$; $wR2 = [\Sigma w(F_o^2 - F_c^2)^2/\Sigma wF_o^4]^{1/2}$

RESULTS AND DISCUSSION

Crystal Structure of the Helicate Complex. The crystal structure of $Cu_2L(ClO_4)_2\cdot0.33DMSO\cdot0.33[Na_2OH(H_2O)(ClO_4)_7]$ is formed by Cu_2L^{4+} cations, perchlorate anions, disordered DMSO molecules, and $Na_2OH(H_2O)(ClO_4)_7$ clusters featuring two Na^+ ions bridged by a disordered perchlorate anion. The asymmetric unit is constituted by two nonequivalent Cu_2L^{4+} cations, one of which is located around a 2-fold crystallographic axis. The two Cu_2L^{4+} ions are very similar and show clear helical arrangements of the ligand around a couple of coordinated metal ions. Figure 2 displays the structures of the two Cu_2L^{4+} cations, in the following indicated as A and B, the latter being the one featuring 2-fold symmetry. Selected bond lengths and angles are listed in Table 2. Two Cu^{2+} ions are located at 3.257(2) and 3.219(1) Å from each other in A and B, respectively. The coordination spheres can be described as highly distorted square pyramids, each defined by the donor atoms of half ligand chain composed, in sequence, of one pyridine ring, one ethylenediamine moiety, and two pyridine rings of the other terpyridine group. The basal sites of the coordination pyramids are occupied by three pyridine and one ethylenediamine nitrogen atoms, which are roughly coplanar, the maximum deviation from the mean planes being found in the A complex (0.201(5) Å for N1 and 0.220(7) Å for N6 in the coordination environments of Cu1 and Cu2, respectively). Moreover, Cu1 and Cu2 are more

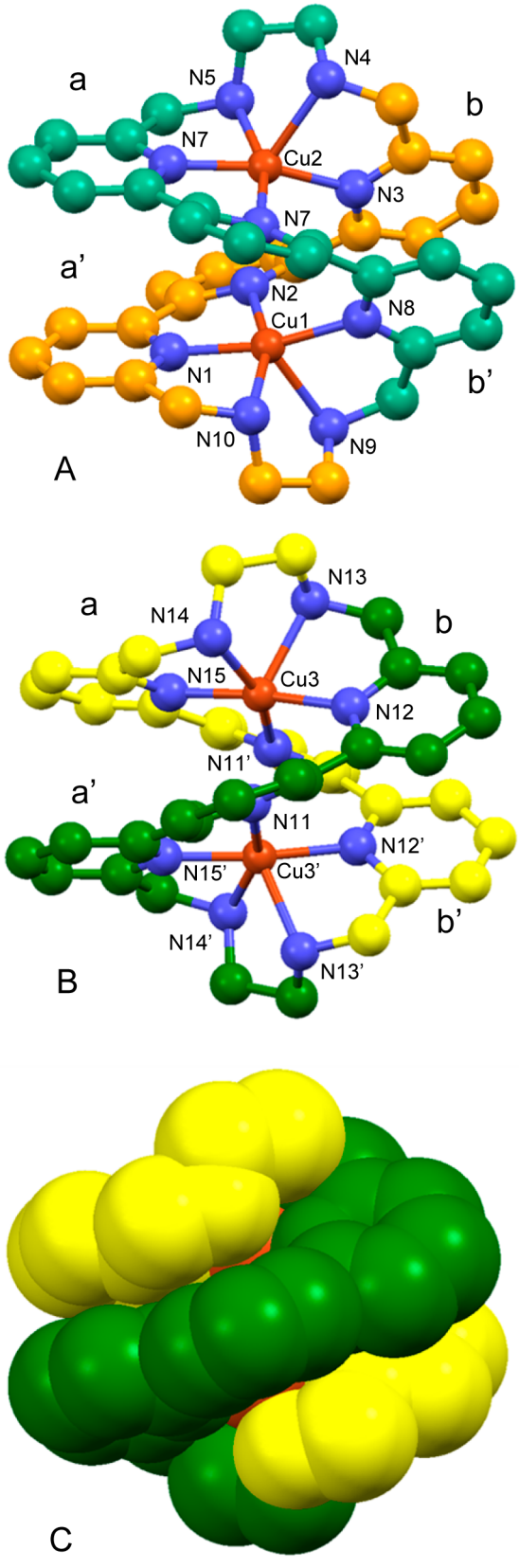

Figure 2. Ball and stick (A, B) drawings of the Cu_2L^{4+} double-strand helicate complex cations observed in the crystal structure of $Cu_2L(ClO_4)_2\cdot0.33DMSO\cdot0.33[Na_2OH(H_2O)(ClO_4)_7]$. (C) Spacefill representation of complex B. ORTEP drawings are available as Supporting Information, Figure S1.

dx.doi.org/10.1021/ic502329s | *Inorg. Chem.* 2014, 53, 12215−12224

Table 2. Selected Bond Lengths (Å) and Angles (deg) for the Helicate Dinuclear Cu^{2+} Complex

complex A		complex B			
Bond Lengths					
Cu3−N11′	2.189(3)[a]	Cu1−N1	1.924(4)	Cu2−N3	2.005(3)
Cu3−N12	2.006(4)	Cu1−N2	2.143(4)	Cu2−N4	2.212(8)
Cu3−N13	2.185(7)	Cu1−N8	1.994(5)	Cu2−N5	2.063(4)
Cu3−N14	2.079(3)	Cu1−N9	2.209(5)	Cu2−N6	1.937(4)
Cu3−N15	1.929(4)	Cu1−N10	2.064(5)	Cu2−N7	2.128(4)
complex A		complex B			
Bond Angles					
N11′−Cu3−N12	102.7(1)	N1−Cu1−N2	80.2(2)	N3−Cu2−N4	79.3(2)
N11′−Cu3−N13	98.0(2)	N1−Cu1−N8	161.0(2)	N3−Cu2−N5	96.4(2)
N11′−Cu3−N14	158.(1)	N1−Cu1−N9	118.0(2)	N3−Cu2−N6	161.6(2)
N11′−Cu3−N15	78.4(1)	N1−Cu1−N10	80.2(2)	N3−Cu2−N7	104.5(2)
N12−Cu3−N13	78.9(2)	N2−Cu1−N8	105.0(2)	N4−Cu2−N5	85.4(2)
N12−Cu3−N14	99.1(2)	N2−Cu1−N9	100.3(1)	N4−Cu2−N6	118.1(2)
N12−Cu3−N15	172.7(2)	N2−Cu1−N10	159.6(1)	N4−Cu2−N7	98.1(2)
N13−Cu3−N14	85.7(2)	N8−Cu1−N9	79.5(2)	N5−Cu2−N6	80.3(2)
N13−Cu3−N15	108.1(2)	N8−Cu1−N10	95.4(2)	N5−Cu2−N7	159.1(2)
N14−Cu3−N15	80.0(2)	N9−Cu1−N10	84.3(1)	N6−Cu2−N7	79.9(2)

[a]Values in parentheses are standard deviation on the last significant figures.

shifted from their own basal planes than Cu3, being located 0.1378(8), 0.133(1), and 0.045(1) Å, respectively, for Cu1, Cu2, and Cu3 out of the respective planes. The apical bond of each coordination pyramid is not at 90° from the corresponding basal plane, as it should be in an ideal square pyramid, but is tilted by 70.2(2)°, 71.3(2)°, and 74.8(2)° for Cu1, Cu2, and Cu3, respectively, due to the short bite of the ethylenediamine chelating unit. Each terpyridine group uses two contiguous pyridine rings to bind one Cu^{2+} ion, while the third ring is coordinated to the other metal ion of the Cu_2L^{4+} complex. The two pyridine rings connected to the same metal center are twisted by 18.8(7)°, 18.2(8)°, and 17.42(7)°, while the remaining pyridine ring forms large dihedral angles of 47.6(7)°, 41.8(8)°, and 40.8(7)° (values referred to Cu1, Cu2, and Cu3, respectively). The double-strand helicate arrangement of the two complexes gives rise to compact structures (Figure 2), which are further stabilized by interstrand $\pi-\pi$ stacking interactions involving two pairs (aa′ and bb′ in Figure 2A,B) of terpyridine rings pertaining to different terpyridine groups. The rings forming the stacked pairs are almost parallel (dihedral angles of 6° for aa′ and 12° for bb′ in complex A and 15° for aa′ and 10° for bb′ in complex B), with ring centroid−ring centroid distance of 3.73(1) and 3.407(7) Å for aa′ and bb′, respectively, in A and 3.71(1) and 3.480(7) Å for aa′ and bb′, respectively, in B.

In conclusion, the ligand is able to form a compact double-strand helicate dinuclear complex with Cu^{2+} by using a TBTB sequence of chelating units, but the definition of the tridentate (T) and bidentate (B) units is operatively different (Figure 3) from the one that was tentatively proposed before these crystal structures were resolved (Figure 1b). The ethylenic chains of the ethylenediamine moieties are more flexible connections than the methylenic ones for the ligand that wraps around the pair of Cu^{2+} ions forming the double helix.

Formation of Cu^{2+} and Zn^{2+} Complexes in Solution. As noted in the Experimental Section, L and HL^+ are characterized by low solubility. Nevertheless, Cu^{2+} and Zn^{2+} (in particular Cu^{2+}) start binding the ligand in very acidic solutions, when it is in higher protonation state, and accordingly, it was possible to perform the speciation of the complex systems over the pH range of 2.5−11 and to determine the relevant stability constants listed in Table 3.

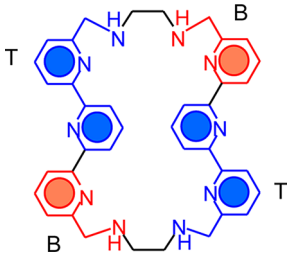

Figure 3. A schematic representation of the effective sequence of tridentate and bidentate binding sites observed in the crystal structure of the double-strand helicate complex.

It was also noted that ligand protonation offers a low competition with metal coordination in acidic solution. As a matter of fact, only six amine groups of the ligand undergo protonation above pH 2.5.[31] The presence of two poorly basic

Table 3. Stability Constants of the Complexes Formed by L with Cu(II) and Zn(II)

reaction[a]	log K	
	Cu^{2+}	Zn^{2+}
$M^{2+} + H_2L^{2+} = MH_2L^{4+}$	16.24(4)[b]	14.31(5)
$M^{2+} + H_3L^{3+} = MH_3L^{5+}$	11.45(6)	10.16(7)
$ML^{2+} + H^+ = MHL^{3+}$	10.21(7)	10.11(7)
$MHL^{3+} + H^+ = MH_2L^{4+}$	8.68(7)	7.10(8)
$MH_2L^{4+} + H^+ = MH_3L^{5+}$	2.90(7)	3.54(8)
$2M^{2+} + H_2L^{2+} = M_2H_2L^{6+}$		19.01(5)
$ML^{2+} + M^{2+} = M_2L^{4+}$	18.32(8)	7.06(7)
$M_2L^{4+} + H^+ = M_2HL^{5+}$	3.58(8)	9.29(7)
$M_2HL^{5+} + H^+ = M_2H_2L^{6+}$		5.56(9)
$M_2L^{4+} + OH^- = M_2L(OH)^{3+}$		4.53(8)

[a]Reaction conditions: 0.1 M NMe_4Cl, 298.1 ± 0.1 K. [b]Values in parentheses are standard deviation on the last significant figures.

dx.doi.org/10.1021/ic502329s | Inorg. Chem. 2014, 53, 12215−12224

terpyridine moieties in close proximity to each other makes some pyridine groups resistant to protonation even in very acidic media. For this reason, EDTA was used as an auxiliary competing ligand to determine the equilibrium constants for Cu^{2+} and Zn^{2+} complexation. Although in the presence of EDTA no evidence of species other than those reported in Table 3 was found in the pH range (2.5−11) of our potentiometric measurements, the high stability of EDTA complexes in very acidic solution (pH < 2) could have covered the formation of complexes by L. Therefore, the possibility that L might be able to coordinate Cu^{2+} and Zn^{2+} in very acidic solution in the absence of EDTA was investigated by means of UV−vis spectra recorded upon addition of increasing amounts of metal ion to ligand solutions. While addition of Zn^{2+} did not affect the spectrum of the ligand at pH 1, indicating that no complexation occurs at such pH, in the case of Cu^{2+} a new set of spectra was generated, according to the formation of a 1:1 metal-to-ligand complex (Figure 4). Reasonably, this complex is

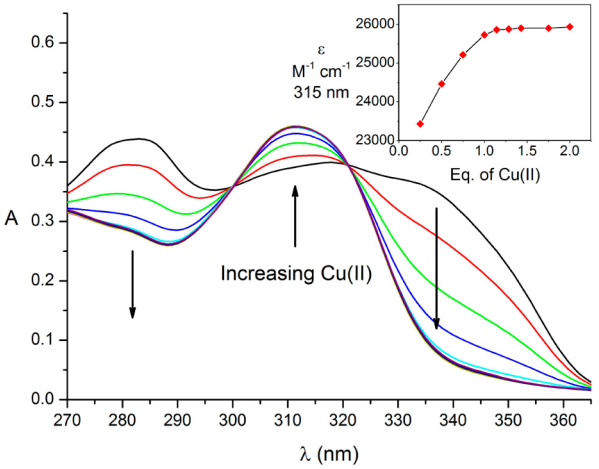

Figure 4. Spectral variations upon addition of Cu^{2+} to a ligand aqueous solution at pH 1. [L] = 2 × 10^{-5} M. (inset) Variation of the molar absorptivity at 315 nm with the equivalents of added Cu^{2+}.

expected to be a mononuclear species with the ligand in a protonation state higher than CuH_3L^{5+}, which is the most protonated mononuclear complex detected in our potentiometric measurements (pH > 2.5).

Despite the peculiar ability of L to bind Cu^{2+} in very acidic solutions, the most striking result disclosed by the equilibrium study is the remarkable ability of L to form binuclear Cu^{2+} complexes, in particular, the double-strand helicate Cu_2L^{4+} complex. As a matter of fact, although the equilibrium constant (log K = 16.24) for the binding of Cu^{2+} by the diprotonated H_2L^{2+} ligand form accounts for the formation of a very stable CuH_2L^{4+} complex, the equilibrium constant for the coordination of the second Cu^{2+} ion is even greater (log K = 18.32 for CuL^{2+} + Cu^{2+} = Cu_2L^{4+}), despite the fact that H_2L^{2+} and CuL^{2+} have the same positive charge but CuL^{2+} contains a lower number of donor atoms available for coordination than H_2L^{2+}. As shown by the distribution diagram of the complexes formed as a function of pH in Figure 5a, in the presence of equimolar amounts of ligand and metal ion, the binuclear Cu_2HL^{5+} and Cu_2L^{4+} complexes are the predominant species around pH 2 and 9.5, respectively. The predisposition of L to form binuclear Cu^{2+} complexes is so high that even in solution containing less than equimolar amount of Cu^{2+}, the binuclear species are still

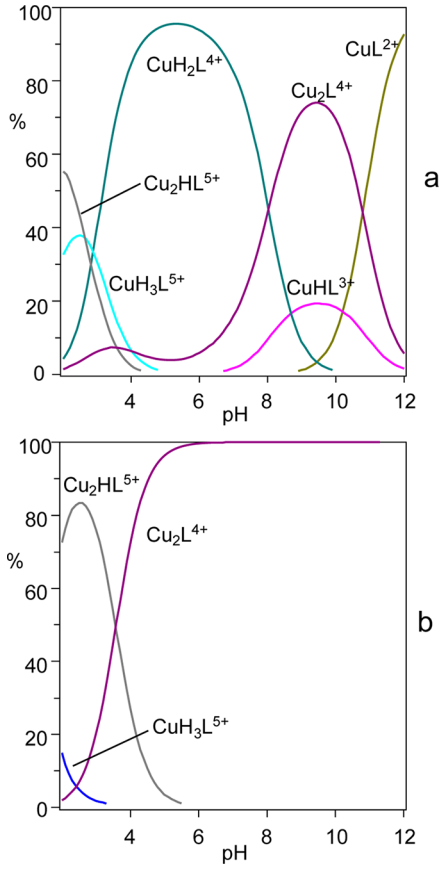

Figure 5. Distribution diagrams of the complex species formed in the system L/Cu^{2+}. (a) [L] = [Cu^{2+}] = 1 × 10^{-3} M; (b) [L] = 1 × 10^{-3} M, [Cu^{2+}] = 2[L]. Percentages are referred to metal ion concentration.

formed in considerable amount. For example, in a solution with a concentration of L twice that of Cu^{2+} ([L] = 2[Cu^{2+}], [L] = 1 × 10^{-3} M) at pH 9.5, ∼60% of metal is still involved in the formation of Cu_2L^{4+}, which is the most abundant species under such conditions (Supporting Information, Figure S2).

The binuclear helicate complex is also very resistant to ligand protonation, being able to form in very acidic solutions. At pH 2, for instance, in a solution containing Cu^{2+} and L in 2:1 molar ratio, the Cu_2HL^{5+} complex is present in 80%, while, at the same pH, Cu_2L^{4+} starts being formed to become the unique species above pH 4 (Figure 5b). As shown by the structure observed in the solid phase (Figure 2), the double-strand Cu_2L^{4+} helicate is stabilized by the formation of strong intramolecular $\pi-\pi$ stacking interactions. Considering the compact structure of this complex (Figure 2C) and the hydrophobic nature of terpyridine groups, it seems very likely that such interactions are maintained in water, contributing to the high stability of the helicate complex. The effect of $\pi-\pi$ stacking interactions in stabilizing the double-strand helicate structures of copper helicates was early evidenced for 2:2 and 3:2 metal-to-ligand Cu^{+} complexes with oligobipyridine ligands containing, respectively, two and three 2,2′-bipyridine subunits,[63] and for 2:2 complexes of Cu^{2+} with quinquepyridine.[64]

Noticeably, along with its high thermodynamic stability, the double-strand helicate complex gives rise to a slow dissociation process in acidic media. At pH 0.71, for instance, it can be evaluated that the time constant for dissociation $1/\tau$ is (4.33 ± 0.01) × 10^{-3} s^{-1} (Figure 6a). Thus, even under such extreme condition, the complex needs more than 10 min to dissociate.

dx.doi.org/10.1021/ic502329s | Inorg. Chem. 2014, 53, 12215−12224

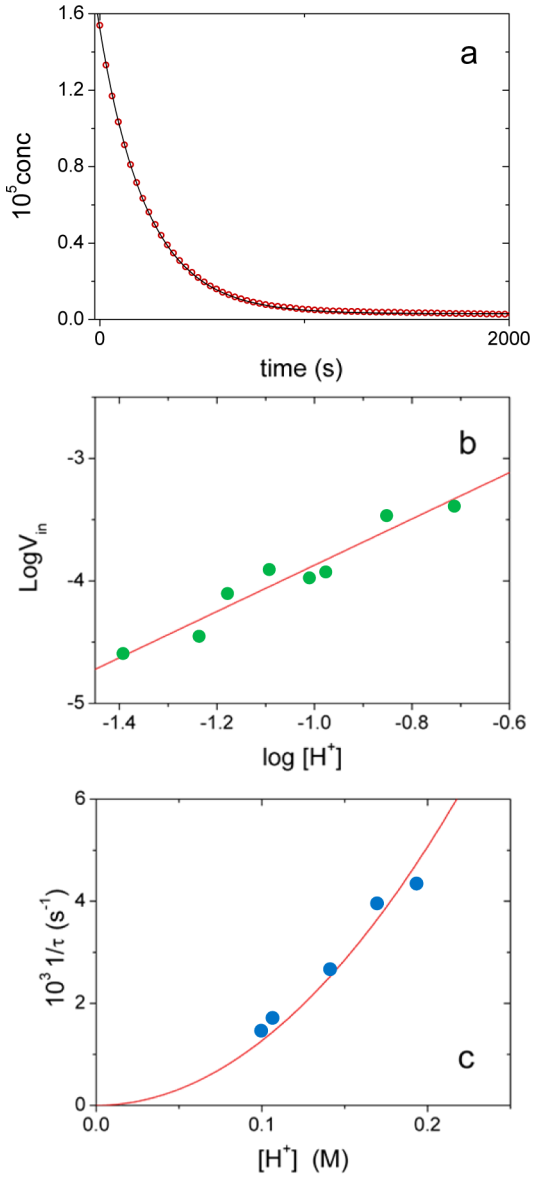

Figure 6. Kinetic analysis of Cu_2L^{4+} dissociation at I = 0.22 M (HCl), 298.1 ± 0.1 K. (a) Kinetic trace related to absorbance variations in time upon addition of H^+ to a preformed binuclear Cu^{2+} complex; pH 0.71, 330 nm, the continuous line is the monoexponential fit of the curve. (b) Dilogarithmic plot for the determination of the reaction order with respect to $[H^+]$; slope = 1.9 ± 0.1. (c) Dependence of the reciprocal time constant, $1/\tau$, on the $[H^+]$ content; the continuous line is the data fit according to a $1/\tau = k[H^+]^2$ function.

The analysis of the initial rates (V_{in}) is shown in Figure 6b. The slope of the dilogarithmic log V_{in} versus log$[H^+]$ plot is 1.9 ± 0.1, indicating that the reaction order for dissociation with respect to H^+ is two. The monoexponential analysis of the kinetic experiments (0.7−1.0 pH range) confirms this result. Inspection of the $1/\tau$ dependence on $[H^+]$ (Figure 6c) shows that this is higher than first order, as a linear trend (first-order kinetics) would yield negative intercepts (negative reaction rates). On this basis, and taking into account the species distribution under the conditions of experiments (Figure 5) and that at pH 1 L forms a protonated mononuclear complex even in the presence of two equivalents of Cu^{2+} (Figure 4), the following dissociation mechanism is proposed.

$$Cu_2L^{4+} + H^+ \rightarrow Cu_2HL^{5+} \quad (1)$$

$$Cu_2HL^{5+} + 2H^+ \rightarrow CuH_3L^{5+} + Cu^{2+} \quad (2)$$

$$CuH_3L^{3+} + nH^+ \rightarrow CuH_{3+n}L^{(3+n)+} \quad (3)$$

Here, steps (1) and (3), concerning protonation processes, are supposed to be very fast, whereas (2) represents the rate-determining copper dissociation step. The kinetic data are thus referred to step (2), and the $1/\tau$ versus $[H^+]$ plot (Figure 6c) can be interpolated according to the eq $1/\tau = k[H^+]^2$ yielding k = 0.12 ± 0.01 M^{-2} s^{-1}, where k is the rate constant of step (2) of the above mechanism. Control spectrophotometric experiments carried out at pH = 4, where step (1) only is supposed to take place, do not display any kinetic trace, confirming the hypothesis that this step is very fast. Kinetic experiments carried out in the 1 ≤ pH ≤ 1.4 range display some deviations from the monoexponential trend that become more significant as the pH increases. This finding is in agreement with the hypothesis that step (2) should occur through the formation of an intermediate species. Note also that additional alternative zero- or first-order dissociation steps cannot be totally ruled out from the reaction mechanism; however, the data indicate that these are at least minor.

In contrast to the great stability and robustness of the binuclear Cu^{2+} complexes, Zn^{2+} is not very prone to form analogous species. As observed for Cu^{2+}, also the stability of the mononuclear Zn^{2+} complexes is fairly high (see for instance log K = 14.31 for $Zn^{2+} + H_2L^{2+} = ZnH_2L^{4+}$, Table 3), but the propensity of the mononuclear complex to add a second metal ion is dramatically lower (log K = 7.06 for $ZnL^{2+} + Zn^{2+} = Zn_2L^{4+}$) than in the case of Cu^{2+} (Table 3). Accordingly, the binuclear complexes of Zn^{2+} become important species in solution only when Zn^{2+} exceeds the concentration of L (Figure 7), but it is not greater than 1.8[L]; otherwise, precipitation of Zn^{2+} hydroxide occurs in the alkaline zone. That is, L is not able to completely bind 2 equiv of Zn^{2+} in water. Furthermore, the equilibrium constant for protonation of Zn_2L^{4+} to form Zn_2HL^{5+} (log K = 9.29, Table 3) is high enough to justify the presence in Zn_2L^{4+} of an aliphatic nitrogen not involved in metal coordination, and even the equilibrium constant for the second protonation step is rather high (log K = 5.56). Moreover, Zn^{2+} complexes are less resistant than Cu^{2+} species to acidic conditions, being completely dissociated at pH 1, and give rise to fast dissociation reactions.

To get further information on these complexation equilibria, we recorded the UV spectra at various pH values of aqueous solution containing L and the metal ions, in 1:1 and 1:2 molar ratios for Cu^{2+}, in 1:1 and 1:1.5 molar ratios for Zn^{2+}. As mentioned previously, the 1:2 molar ratio for Zn^{2+} would cause metal hydroxide precipitation in alkaline solution. In the case of Cu^{2+}, however, the spectra are not very informative. The most relevant features are a red shift of ∼10 nm, observed for the binuclear complexes relative to mononuclear ones, and the formation of a small peak at 282 nm on increasing the pH in the presence of L and Cu^{2+} in 1:2 molar ratio (Supporting Information, Figure S3).

In the case of Zn^{2+}, due to the weakness of the complexes in acidic solution, the spectral variation with pH evidences the formation of complexes with disappearance of the 280 nm band, typical of the protonated species of the ligand (Supporting Information, Figure S4), and formation of a band at about 315 nm typical of the complex. Such spectra

dx.doi.org/10.1021/ic502329s | Inorg. Chem. 2014, 53, 12215−12224

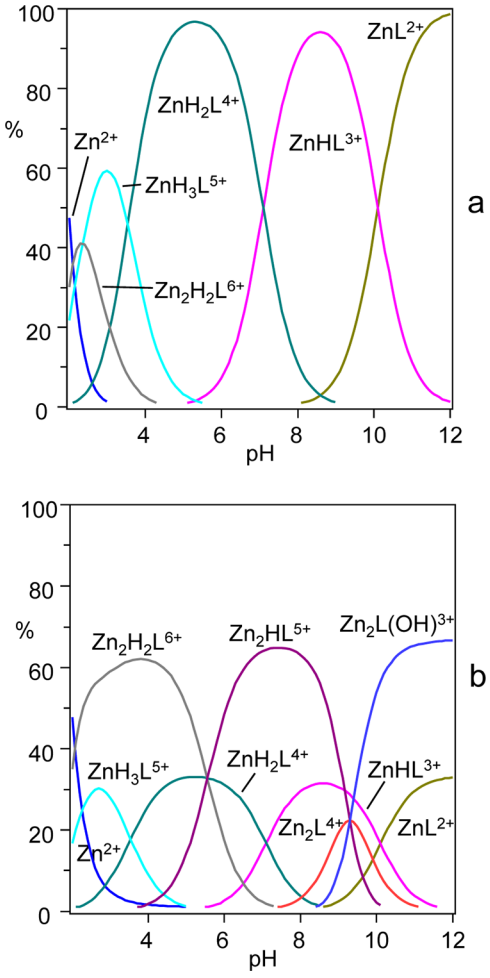

Figure 7. Distribution diagrams of the complex species formed in the system L/Zn^{2+}. (a) [L] = [Zn^{2+}] = 1×10^{-3} M; (b) [L] = 1×10^{-3} M, [Zn^{2+}] = 1.5[L]. Percentages refer to metal ion concentration.

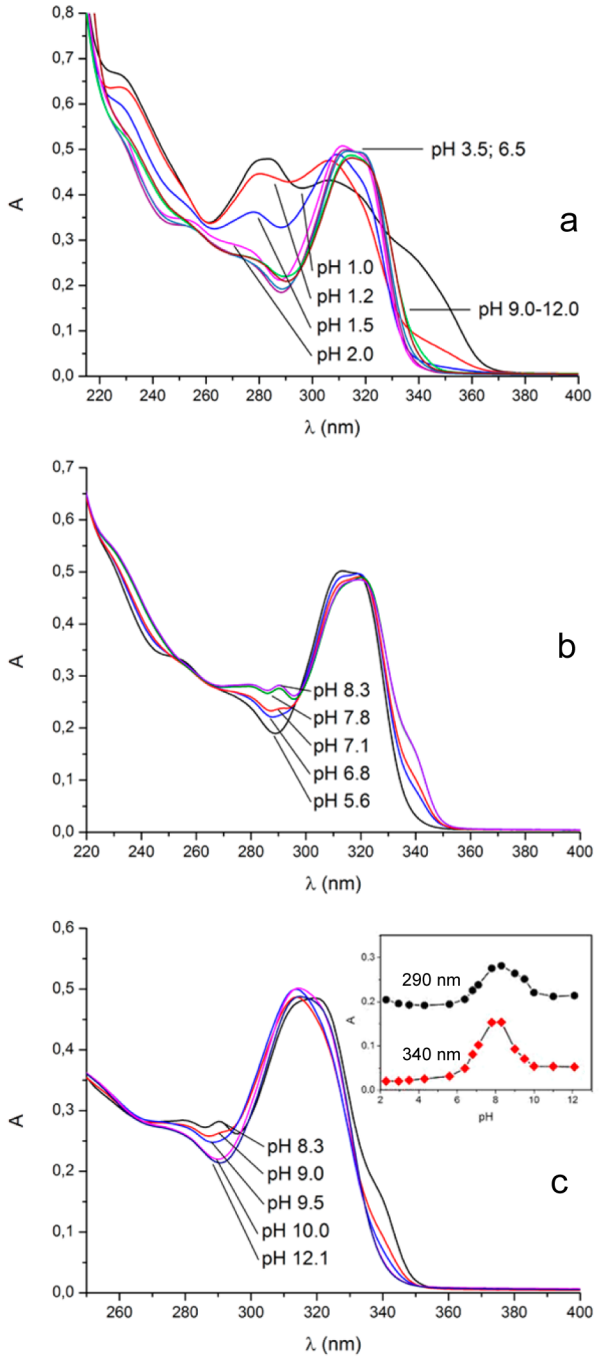

Figure 8. UV spectra, recorded at different pH, of aqueous solutions containing L and Zn^{2+} in 1:1 (a) and 1:1.5 (b, c) molar ratios. [L] = 2×10^{-5} M. (inset) Variation of the 290 and 340 nm absorbances with pH.

recorded in the acidic region are shown in Figure 8a and Supporting Information, Figure S5 for 1:1 and 1:1.5 ligand-to-metal molar ratios, respectively. In this pH region, the spectral variations are similar for both molar ratios, since the complex species involved are the same in both systems, although they are formed in different proportions, and because the complex absorption band at 315 nm is not very sensible to the formation of mono- or binuclear complexes (Figure 8). The largest variation in complex spectra is observed for 1:1.5 ligand-to-metal molar ratio at ~290 nm, where a small peak emerges in a limited pH range and at ~340 nm. A plot of the 290 and 340 nm absorbances versus pH (inset of Figure 8) shows a transient increase in the pH range of 6–10. Since a similar spectral feature was not observed for 1:1 ligand-to-metal molar ratio, such transient increase of absorbance must be due to the transient formation of a binuclear complex in the same pH range, the only option being Zn_2HL^{5+} (Figure 7). Apparently, protonation of Zn_2L^{4+} to form Zn_2HL^{5+} affects the overall interaction of the terpyridine groups with the pair of metal ions, while the successive protonation giving rise to $Zn_2H_2L^{6+}$ restores the original situation.

More spectroscopic information was obtained by using an organic solvent to follow the complexation equilibria, thus eliminating all complications arising from the low solubility of L and from the formation of zinc hydroxide occurring in water for 1:2 ligand-to-metal molar ratio. The choice of the solvent, a DMSO/$CHCl_3$ 9:1 (v/v) mixture, was a compromise between the use of a solvent (DMSO) able to dissolve the highly charged M_2L^{4+} complexes and a solvent ($CHCl_3$) able to dissolve L. As shown in Figure 9a, the addition of increasing amounts of Cu^{2+} to a solution of L in this solvent produces a decrease of the UV absorption band centered at 274 nm and a simultaneous increase of the 320 nm peak. The profiles of the 274 and 320 nm absorbances variations with the equivalents of added metal ion (for the 320 nm absorbance see inset of Figure 9a), characterized by two net changes of slope, accounts for two

dx.doi.org/10.1021/ic502329s | Inorg. Chem. 2014, 53, 12215–12224

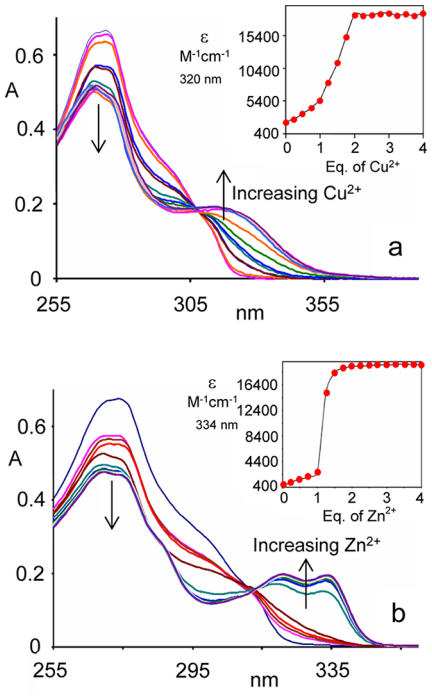

Figure 9. UV spectra of L (9.67×10^{-6} M) upon addition of increasing amounts of Cu^{2+} (a) and Zn^{2+} (b). (a, inset) Variation of the 320 nm molar absorptivity (ε) with increasing Cu^{2+}. (b, inset) Variation of the 334 nm molar absorptivity (ε) with the equivalents of added Zn^{2+}. Solvent: DMSO/$CHCl_3$ 9:1 (v/v).

consecutive complexation stages occurring with the formation of very stable complexes with 1:1 and 2:1 metal-to-ligand stoichiometries. The appearance and continuous growth of the 320 nm peak since the first additions of metal ion indicates that terpyridine rings are involved in both complexation stages, although a larger involvement is observed in the second one when the helicate Cu_2L^{4+} is formed.

Also the addition of Zn^{2+} to a solution of L in the organic solvent produces a decrease of the 274 nm band, while a new structured band, typical of Zn^{2+} complexes with terpyridine ligands, appears with a maximum at 334 nm (Figure 9b). A plot of the 334 nm absorbance as a function of the equivalents of added Zn^{2+} (the same behavior is shown by the 274 nm band) shows that the formation of a stable complex with 1:1 stoichiometry is followed by the weaker coordination of a second metal ion (inset of Figure 9b) in agreement with the results obtained in water. Interestingly, the addition of the first equivalent of Zn^{2+} gives rise to modest modifications of the 334 nm absorbance, which is very sensible to terpyridine complexation, revealing that the terpyridine groups are less involved in the binding of the metal ion in the ZnL^{2+} complex. Conversely, the binding of the second Zn^{2+} ion to form Zn_2L^{4+} is accompanied by a large absorbance increase (inset of Figure 9b) accounting for an intense involvement of terpyridine groups.

The fluorescence spectrum of L, obtained upon excitation of the ligand at 313 nm in the same organic solvent, is characterized by a weak emission band with a maximum at 340 nm (Figure 10). As previously observed for other polyamine ligands containing terpyridine groups,[10] the aliphatic nitrogen atoms can operate, through their lone pairs, a photoinduced electron transfer (PET) toward the excited terpyridine chromophore quenching its emission. This is the

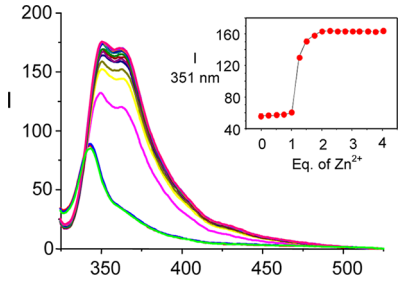

Figure 10. Fluorescence emission spectra recorded upon excitation at 313 nm of a solution containing L (9.67×10^{-6} M,) and increasing amounts of Zn^{2+} in a DMSO/$CHCl_3$ 9:1 mixture. The green spectrum was recorded in the absence of metal. (inset) Variation of the 351 nm emission intensity with the equivalents of added Zn^{2+}. Intensities are in arbitrary unit. Solvent: DMSO/$CHCl_3$ 9:1 (v/v).

reason why L is poorly emissive. When the lone pairs of these aliphatic nitrogen atoms are involved in proton or metal ion binding, they are no longer available for the PET process, and the terpyridine groups can manifest their emissive properties. Accordingly, L displays a significant enhancement of emission upon coordination to Zn^{2+} (Figure 10). This enhancement, however, is modest upon addition of the first equivalent of Zn^{2+}, while it becomes much larger as the second equivalent is added. This means that after the coordination of the first Zn^{2+} ion, the ZnL^{2+} complex still contains enough uncoordinated aliphatic amine groups to perform an efficient PET process. Then, on the basis of fluorescence emission and absorption spectra, we can conclude that in the ZnL^{2+} complex the metal ion should be coordinated to an ethylenediamine group and few terpyridine rings, while in the binuclear Zn_2L^{4+} complex all or about all the donor atoms should be involved.

Emission spectra recorded upon addition of increasing amounts of Cu^{2+} to a solution of L in the organic solvent showed a progressive quenching of the fluorescence emission as expected for this metal ion (Supporting Information, Figure S6).[65]

In conclusion, the macrocyclic ligand L, despite its relatively small ring dimensions, is able to assemble, upon coordination to two Cu^{2+} ions, a compact double-strand macrocyclic helicate complex[66] characterized by high thermodynamic stability and significant inertness toward acid-promoted demetalation processes. Intramolecular $\pi-\pi$ stacking of pyridine rings, already observed in the structure of the H_4L^{4+} metal-free cation,[31] plays an important role in the stabilization of the double helix and favors its spontaneous assembly from the components. Self-organization of these components occurs through the combined action of coordinative and stacking interactions, the Cu^{2+} ions holding together the two intramolecular stacked strands of L as hydrogen bonding of stacked base-pairs maintains the double helix in nucleic acids. The relevance of intramolecular stacking interactions for the formation of the helicate Cu_2L^{4+} complex is highlighted by the occurrence that the completely aliphatic polyamine macrocycle 1,4,7,10,13,16,19,21,24,27,30-decaazacyclotetradecane ([30]aneN_{10}), which is similar to L regarding number of nitrogen donors and ring size, forms stable binuclear M_2L^{4+} complexes with several metal ions (M = Cu^{2+}, Zn^{2+}, Cd^{2+}, Ni^{2+}) that do not display any tendency to assume a helicate conformation.[67]

Thermodynamic and kinetic information about the Zn^{2+} complexes do not show any of the characteristic found for

the Cu^{2+} ones, although no experimental evidence was found that can exclude a double-strand helicate structure for the binuclear Zn_2L^{4+} complex.

■ ASSOCIATED CONTENT

Supporting Information

X-ray crystallographic files in CIF format for $Cu_2L(ClO_4)_2 \cdot 0.33DMSO \cdot 0.33[Na_2OH(H_2O)(ClO_4)_7]$ complex. ORTEP drawings of the Cu_2L^{4+} double-strand helicate complex cations. Distribution diagram of the Cu^{2+} complexes formed in the presence of 2 equiv of L. UV absorption and emission spectra of complexes and/or free L in water and in DMSO/$CHCl_3$ 9:1 (v/v) solution. This material is available free of charge via the Internet at http://pubs.acs.org. CCDC 1025211 contains the supplementary crystallographic data for $Cu_2L(ClO_4)_2 \cdot 0.33DMSO \cdot 0.33[Na_2OH(H_2O)(ClO_4)_7]$.

■ AUTHOR INFORMATION

Corresponding Author

*E-mail: antonio.bianchi@unifi.it.

Notes

The authors declare no competing financial interest.

The staircase architecture "Umschreibung" shown in the TOC was designed by Olafur Eliasson. The staircase was completed in 2004 and was placed in the courtyard of KPMG in Munich, Germany.

■ REFERENCES

(1) Zak, B.; Baginsky, E. S.; Epstein, E.; Weiner, L. M. *Clin. Chim. Acta* **1970**, *29*, 77−82.
(2) Zak, B.; Baginsky, E. S.; Epstein, E.; Weiner, L. M. *Clin. Toxicol.* **1971**, *4*, 621−629.
(3) McWhinnie, W. R.; Miller, J. D. *Adv. Inorg. Chem. Radiochem.* **1969**, *12*, 135−215.
(4) Constable, E. C. *Adv. Inorg. Chem. Radiochem.* **1986**, *30*, 69−121.
(5) Constable, E. C.; Holmes, J. M.; McQueen, R. C. S. *J. Chem. Soc., Dalton Trans.* **1987**, 5−8.
(6) Sauvage, J. P.; Collin, J. P.; Chambron, J. C.; Guillerez, S.; Coudret, C.; Balzani, V.; Barigelletti, F.; De Cola, L.; Flamigni, L. *Chem. Rev.* **1994**, *94*, 993−1019.
(7) Balzani, V.; Venturi, M.; Credi, A. *Molecular Devices and Machines;* Wiley−VCH: Weinheim, Germany, 2003.
(8) Lindoy, L. F.; Atkinson, I. M. *Self-Assembly in Supramolecular Systems;* Royal Society of Chemistry: Cambridge, U.K., 2000.
(9) Hofmeier, H.; Schubert, H. S. *Chem. Soc. Rev.* **2004**, *33*, 373−399.
(10) Bazzicalupi, C.; Bencini, A.; Bianchi, A.; Danesi, A.; Faggi, E.; Giorgi, C.; Santarelli, S.; Valtancoli, B. *Coord. Chem. Rev.* **2008**, *252*, 1052−1068.
(11) Létinois-Halbes, U.; Hanss, D.; Beierle, J. M.; Collin, J.-P.; Sauvage, J.-P. *Org. Lett.* **2005**, *7*, 5753−5756.
(12) Weber, N.; Hamann, C.; Kern, J.-M.; Sauvage, J.-P. *Inorg. Chem.* **2003**, *42*, 6780−6792.
(13) Kern, J.-M.; Raehm, L.; Sauvage, J.-P.; Divisia-Blohorn, B.; Vidal, P.-L. *Inorg. Chem.* **2000**, *39*, 1555−1560.
(14) Raehm, L.; Kern, J.-M.; Sauvage, J.-P. *Chem.—Eur. J.* **1999**, *5*, 3310−3317.
(15) Collin, J.-P.; Mobian, P.; Sauvage, J.-P.; Sour, A.; Yan, Y.-M.; Willner, I. *Aust. J. Chem.* **2009**, *62*, 1231−1237.
(16) Loren, J. C.; Gantzel, P.; Lindenb, A.; Siegel, J. S. *Org. Biomol. Chem.* **2005**, *3*, 3105−3116.
(17) Hamann, C.; Kern, J.-M.; Sauvage, J.-P. *Inorg. Chem.* **2003**, *42*, 1877−1883.
(18) Rapenne, G.; Dietrich-Buchecker, C.; Sauvage, J.-P. *J. Am. Chem. Soc.* **1999**, *121*, 994−1001.
(19) Cheng, H. N.; Leigh, D. A.; Maffei, F.; McGonigal, P. R.; Slawin, A. M. Z.; Wu, J. *J. Am. Chem. Soc.* **2011**, *133*, 12298−12303.
(20) Loren, J. C.; Yoshizawa, M.; Haldimann, R. F.; Linden, A.; Siegel, J. S. *Angew. Chem., Int. Ed.* **2003**, *42*, 5701−5075.
(21) Constable, E. C.; Holmes, J. M.; McQueen, R. C. S. *J. Chem. Soc., Dalton Trans.* **1987**, 5−8.
(22) Constable, E. C.; Lewis, J.; Liptrot, M. C.; Raithby, P. R.; Schroeder, M. *Polyhedron* **1983**, *2*, 301−302.
(23) Marquez, V. E.; Anacona, J. R. *Transition Metal Chem.* **2004**, *29*, 66−69.
(24) Marquez, V. E.; Anacona, J. R. *Polyhedron* **1997**, *16*, 2375−2379.
(25) Marquez, V. E.; Anacona, J. R.; Loroño, D. *Polyhedron* **2004**, *23*, 1317−1323.
(26) Marquez, V. E.; Anacona, J. R.; Rodriguez Barbarin, C. *Polyhedron* **2001**, *20*, 1885−1890.
(27) Marquez, V. E.; Anacona, J. R. *Transition Metal Chem.* **2000**, *25*, 188−191.
(28) Deslandes, S.; Galaup, C.; Poole, R.; Mestre-Voegtlé; Stéphanie Soldevila, S.; Leygue, N.; Bazin, H.; Lamarque, L.; Picard, C. *Org. Biomol. Chem.* **2012**, *10*, 8509−8523.
(29) Galaup, C.; Couchet, J.-M.; Bedel, S.; Tisnés, P.; Picard, C. *J. Org. Chem.* **2005**, *70*, 2274−2284.
(30) Galaup, C.; Couchet, J.-M.; Picard, C.; Tisnés, P. *Tetrahedron Lett.* **2001**, *42*, 6275−6278.
(31) Bazzicalupi, C.; Bencini, A.; Bianchi, A.; Faggi, E.; Giorgi, C.; Santarelli, S.; Valtancoli, B. *J. Am. Chem. Soc.* **2008**, *130*, 2440−2441.
(32) Bazzicalupi, C.; Bencini, A.; Bianchi, A.; Danesi, A.; Faggi, E.; Giorgi, C.; Lodeiro, C.; Oliveira, E.; Pina, F.; Valtancoli, B. *Inorg. Chim. Acta* **2008**, *361*, 3410−3419.
(33) Bazzicalupi, C.; Bencini, A.; Bianchi, A.; Danesi, A.; Giorgi, C.; Lodeiro, C.; Pina, F.; Santarelli, S.; Valtancoli, B. *Chem. Commun.* **2005**, 2630−2632.
(34) Kwong, H.-L.; Wonga, W.-L.; Lee, C.-S.; Yeung, C.-T.; Teng, P.-F. *Inorg. Chem. Commun.* **2009**, *12*, 815−818.
(35) Wong, W.-L.; Huang, K.-H.; Teng, P.-F.; Lee, C.-S.; Kwong, H.-L. *Chem. Commun.* **2004**, 384−385.
(36) Bazzicalupi, C.; Bencini, A.; Bianchi, A.; Borsari, L.; Danesi, A.; Giorgi, C.; Mariani, P.; Pina, F.; Santarelli, S.; Valtancoli, B. *Dalton Trans.* **2006**, 5743−5752.
(37) Verdejo, B.; Blasco, S.; González, J.; García-España, E.; Gaviña, P.; Tatay, S.; Doménech, A.; Doménech-Carbó, M. T.; Jiménez, H. R.; Soriano, C. *Eur. J. Inorg. Chem.* **2008**, 84−97.
(38) García-España, E.; Gaviña, P.; Latorre, J.; Soriano, C.; Verdejo, B. *J. Am. Chem. Soc.* **2004**, *126*, 5082−5083.
(39) Belfrekh, N.; Dietrich-Buchecker, C.; Sauvage, J.-P. *Inorg. Chem.* **2000**, *39*, 5169−5172.
(40) Lehmann, U.; Schlüter, A. D. *Eur. J. Org. Chem.* **2000**, 3483−3487.
(41) Grave, C.; Lentz, D.; Schäfer, A.; Samorì, P.; Rabe, J. P.; Franke, F.; Schlüter, A. D. *J. Am. Chem. Soc.* **2003**, *125*, 6907−6918.
(42) Baxter, P. N. W. *Chem.—Eur. J.* **2003**, *9*, 5011−5022.
(43) Baxter, P. N. W.; Gisselbrecht, J.-P.; Karmazin-Brelot, L.; Varnek, A.; Allouche, L. *Chem.—Eur. J.* **2013**, *19*, 12336−12349.
(44) Marquis, A.; Smith, V.; Harrowfield, J.; Lehn, J.-M.; Herschbach, H.; Sanvito, R.; Leize-Wagner, E.; Van Dorsselaer, A. *Chem.—Eur. J.* **2006**, *12*, 5632−5641.
(45) Hasenknopf, B.; Lehn, J.-M.; Baum, G.; Fenske, D. *Proc. Natl. Acad. Sci. U.S.A.* **1996**, *93*, 1397−1400.
(46) Yeung, C.-T.; Yeung, H.-L.; Tsang, C.-S.; Wong, W.-Y.; Kwong, H.-L. *Chem. Commun.* **2007**, 5203−5205.
(47) Constable, E. C.; Housecroft, C. E.; Neuburger, M.; Schaffner, S.; Shardlow, E. J. *Inorg. Chem. Commun.* **2005**, *8*, 743−745.
(48) Baum, G.; Constable, E. C.; Fenske, D.; Housecroft, C. E.; Kulke, T.; Neuburger, M.; Zehnder, M. *J. Chem. Soc., Dalton Trans.* **2000**, 945−959.
(49) Constable, E. C.; Kulke, T.; Neuburger, M.; Zehnder, M. *Chem. Commun.* **1997**, 489−490.
(50) El-ghayouy, A.; Harriman, A.; De Cian, A.; Fischer, J.; Ziessel, R. *J. Am. Chem. Soc.* **1998**, *120*, 9973−9974.
(51) Potts, K. T.; Keshavarz-K, M.; Tham, F. S.; Abruila, H. D.; Aranat, C. *Inorg. Chem.* **1993**, *32*, 4450−4456.

(52) Andrés, A.; Bazzicalupi, C.; Bianchi, A.; García-España, E.; Luis, S. V.; Miravet, J. F.; Ramírez, J. A. *J. Chem. Soc., Dalton Trans.* **1994**, 2995−3004.
(53) Bazzicalupi, C.; Biagini, S.; Bianchi, A.; Faggi, E.; Gratteri, P.; Mariani, P.; Pina, F.; Valtancoli, B. *Dalton Trans.* **2010**, *39*, 10128−10136.
(54) Bazzicalupi, C.; Bencini, A.; Berni, E.; Bianchi, A.; Fornasari, P.; Giorgi, C.; Valtancoli, B. *Inorg. Chem.* **2004**, *43*, 6255−6265.
(55) García-España, E.; Latorre, J.; Luis, S. V.; Miravet, J. F.; Pozuelo, P. E.; Ramírez, J. A.; Soriano, C. *Inorg. Chem.* **1996**, *35*, 4591−4596.
(56) Bazzicalupi, C.; Bianchi, A.; Giorgi, C.; Gratteri, P.; Mariani, P.; Valtancoli, B. *Inorg. Chem.* **2013**, *52*, 2125−2137.
(57) Gran, G. *Analyst (London, U.K.)* **1952**, *77*, 661−671.
(58) Gans, P.; Sabatini, A.; Vacca, A. *Talanta* **1996**, *43*, 1739−1753.
(59) Smith, R. M.; Martell, A. E.; *NIST Stability Constants Database,* Version 4.0; National Institute of Standards and Technology: Gaithersburg, MD, 1997.
(60) *CrysAlisPro,* Version 1.171.35.11; Agilent Technologies: Santa Clara, CA.
(61) Altomare, A.; Cascarano, G.; Giacovazzo, C.; Guagliardi, A.; Burla, M. C.; Polidori, G.; Camalli, M. *J. Appl. Crystallogr.* **1994**, *27*, 435−436.
(62) Sheldrick, G. M. *Acta Crystallogr.* **2008**, *A64*, 112−122.
(63) Lehn, J.-M.; Rigault, A.; Siegel, J.; Harrowfield, J.; Chevrier, B.; Moras, D. *Proc. Natl. Acad. Sci. U. S. A.* **1987**, *84*, 2565−2569.
(64) Constable, E. C.; Drew, M. G. B.; Ward, M. D. *J. Chem. Soc., Chem. Commun.* **1987**, 1600−1601.
(65) Bencini, A.; Bernardo, M. A.; Bianchi, A.; García-España, E.; Giorgi, C.; Luis, S.; Pina, F.; Valtancoli, B. Sensing Cations and Anions by Luminescent Polyamine Receptors in Solution. In *Advances in Supramolecular Chemistry;* Gokel, G., Ed.; Cerberus Press: Miami, FL, 2002; Vol. *8*.
(66) Examples of helicate complexes assembled within a macrocyclic ligand: (a) Campbell, V. E.; de Hatten, X.; Delsuc, N.; Kauffmann, B.; Huc, I.; Nitschke, J. R. *Chem.—Eur. J.* **2009**, *15*, 6138−6142. (b) Hutin, M.; Schalley, C. A.; Bernardinelli, G.; Nitschke, J. R. *Chem.—Eur. J.* **2006**, *12*, 4069−4076. (c) Matthews, R. W.; McPartlin, M.; Scowen, I. J. *J. Chem. Soc., Dalton Trans.* **1997**, 2861−2864. (d) Fenton, D. E.; Matthews, R. W.; McPartlin, M.; Murphy, B. P.; Scowel, I. J.; Tasker, P. A. *J. Chem. Soc., Dalton Trans.* **1996**, 3421−3427. (e) Fenton, D. E.; Matthews, R. W.; McPartlin, M.; Murphy, B. P.; Scowel, I. J.; Tasker, P. A. *J. Chem. Soc., Chem. Comm.* **1994**, 1391−1392.
(67) (a) Bencini, A.; Bianchi, A.; García-España, E.; Giusti, M.; Mangani, S.; Micheloni, M.; Orioli, P.; Paoletti, P. *Inorg. Chem.* **1987**, *26*, 1243−1247. (b) Bencini, A.; Bianchi, A.; García-España, E.; Mangani, S.; Micheloni, M.; Orioli, P.; Paoletti, P. *Inorg. Chem.* **1988**, *27*, 1104−1107. (c) Bencini, A.; Bianchi, A.; Castelló, M.; Di Vaira, M.; García-España, E.; Micheloni, M.; Paoletti, P. *Inorg. Chem.* **1989**, *28*, 347−351. (e) Bencini, A.; Bianchi, A.; Castelló, M.; Dapporto, P.; Faus, J.; García-España, E.; Micheloni, M.; Paoletti, P.; Paoli, P. *Inorg. Chem.* **1989**, *28*, 3175−3181.